

## How simulated fluence of photons from terrestrial gamma ray flashes at aircraft and balloon altitudes depends on initial parameters

R. S. Hansen,<sup>1,2</sup> N. Østgaard,<sup>1,2</sup> T. Gjesteland,<sup>1,2</sup> and B. Carlson<sup>1,2</sup>

Received 8 August 2012; revised 21 November 2012; accepted 24 January 2013; published 3 May 2013.

[1] Up to a few years ago, terrestrial gamma ray flashes (TGFs) were only observed by spaceborne instruments. The aircraft campaign ADELE was able to observe one TGF, and more attempts on aircraft observations are planned. There is also a planned campaign with stratospheric balloons, COBRAT. In this context an important question that arises is what count rates we can expect and how these estimates are affected by the initial properties of the TGFs. Based on simulations of photon propagation in air we find the photon fluence at different observation points at aircraft and balloon altitudes. The observed fluence is highly affected by the initial parameters of the simulated TGFs. One of the most important parameters is the number of initial photons in a TGF. In this paper, we give a semi-analytical approach to find the initial number of photons with an order of magnitude accuracy. The resulting number varies over several orders of magnitude, depending mostly on the production altitude of the TGF. The initial production altitude is also one of the main parameters in the simulations. Given the same number of initial photons, the fluence at aircraft and balloon altitude from a TGF produced at 10 km altitude is 2–3 orders of magnitude smaller than a TGF originating from 20 km altitude. Other important parameters are altitude distribution, angular distribution and amount of feedback. The differences in altitude, altitude distribution and amount of feedback are especially important for the fluence of photons observed at altitudes less than 20 km, and for instruments with a low-energy threshold larger than 100 keV. We find that the maximum radius of observation is 14 km for a TGF with the intensity of an average RHESSI TGF is smaller than the results reported by Smith et al. (2011), and our results support the conclusion in Gjesteland et al. (2012) and Østgaard et al. (2012) that TGFs probably are a more common phenomenon than previously reported.

**Citation:** Hansen, R. S., N. Østgaard, T. Gjesteland, and B. Carlson (2013), How simulated fluence of photons from terrestrial gamma ray flashes at aircraft and balloon altitudes depends on initial parameters, *J. Geophys. Res. Space Physics*, 118, 2333–2339, doi:10.1002/jgra.50143.

### 1. Introduction

[2] Terrestrial gamma ray flashes (TGFs) are short bursts of high energy radiation originating from the Earth's atmosphere and observed from space. The radiation is produced, through the bremsstrahlung process, by energetic electrons that are accelerated by relativistic runaway electrons in strong electric fields. The TGFs are found to be closely connected to thunderstorms and lightning discharges [Inan et al., 1996; Cohen et al., 2010; Shao et al., 2010], so the electric fields are expected to be located in or around thunderstorms.

[3] From spectral analyses of the TGFs seen from space, TGFs have been found to have production altitudes between 15 and 20 km [Dwyer and Smith, 2005; Gjesteland et al., 2010]. There might be TGFs produced at lower altitudes, but due to atmospheric attenuation they will not be detectable from space. Dwyer and Smith [2005] showed that an average RHESSI TGF could be fairly accurately modeled by assuming  $10^{17}$  initial photons produced at 15 km altitude. Østgaard et al. [2012] have suggested that there might exist TGFs with intensities down to  $10^{12}$  initial photons.

[4] Several studies have also aimed at finding the initial angular distribution of the photons in a TGF. Gjesteland et al. [2011] used TGF and lightning observations together with simulations and found the observations to be consistent with an isotropic angular distribution inside a cone with half angle between  $30^\circ$  and  $40^\circ$ . Hazelton et al. [2009] used an anisotropic angular distribution out to 90 degrees and found the best fit to be for a beam with a half maximum at  $35^\circ$  (read out from Figure 2b of Hazelton et al. [2009]).

<sup>1</sup>Department of Physics and Technology, University of Bergen, Bergen, Norway.

<sup>2</sup>Birkeland Centre for Space Science, N-5020 Bergen, Norway

Corresponding author: R. S. Hansen, Department of Physics and Technology, Allegt. 55, N-5007, Bergen, Norway. (Ragnhild.hansen@ift.uib.no)

©2013. American Geophysical Union. All Rights Reserved.  
2169-9380/13/10.1002/jgra.50143

[5] So far, most observations of TGFs have been obtained by spaceborne instruments. The first observations were made by the Burst and Transient Source experiment (BATSE) on board the Compton Gamma Ray Observatory (CGRO) [Fishman, 1994]. During the last 10 years, observations have also been made by Reuven Ramaty High Energy Solar Spectroscopic Imager (RHESSI) [Smith *et al.*, 2005], FERMI [Briggs, 2010], and AGILE [Marisaldi, 2010].

[6] In 2009, an effort to observe TGFs using aircraft-borne instruments was carried out [Smith, 2011a]. During 37 hrs of observations the ADELE instrument detected only one event [Smith, 2011b]. During the flight time, there were more than 1000 lightning discharges closer than 10 km from the aircraft. Smith [2011a] also made a simulation and calculation of the expected number of TGFs. Due to the very few detected events, they concluded that only 0.1–1% of all flashes produce TGFs and that the TGF intensities cannot follow a power law distribution below 1/100 of the average RHESSI TGFs. However, a recent study by Østgaard *et al.* [2012] based on Fermi and RHESSI TGFs as well as the non-detection by ADELE argued that one cannot rule out that all lightning produce TGFs. This is also supported by the findings of more TGFs in the RHESSI data [Gjesteland *et al.*, 2012] and in the GBM Fermi data [Østgaard *et al.*, 2012].

[7] In this paper, we show the results of a simulation of photon fluence at aircraft altitudes as well as at balloon altitudes. As should be clear from this introduction, the constraints obtained from observations still open up for a broad variation of initial conditions, and we show that the resulting fluence is highly dependent on these initial conditions. We also show that the number of initial photons in a TGF seen from space is dependent on the initial conditions used in the simulation.

## 2. Monte Carlo Simulations

[8] The simulation used to find the expected detection rates is based on the Monte Carlo model developed by Østgaard *et al.* [2008]. This model is a more simple model than for instance GEANT or the model of Dwyer [2012], but Østgaard *et al.* [2008] found good correspondence between this model and GEANT. The model propagates photons through the atmosphere in length steps. The density of the atmosphere is approximated by an exponential fit to MSIS data. The initial photons are given an initial energy ( $E$ ), altitude, and direction and are propagated through the atmosphere. The model takes Compton scattering, photoelectric absorption, and pair production into account. The Compton electrons are not taken into account, the photons produced by bremsstrahlung from the electron and positron after pair production is not taken into account, and the positron is assumed to annihilate at the same position as the production of the positron. Østgaard *et al.* [2008] showed that this simplification gives about 7% less photons, in the energy range below 80 keV. As the lower energy threshold for instruments is typically in the range from 200 to 400 keV, the simplification will not affect our results significantly.

[9] We have used 100 million initial photons with an initial energy spectrum as a  $1/E$  spectrum with a cutoff at 40 MeV for all simulations. This is the hardest energy

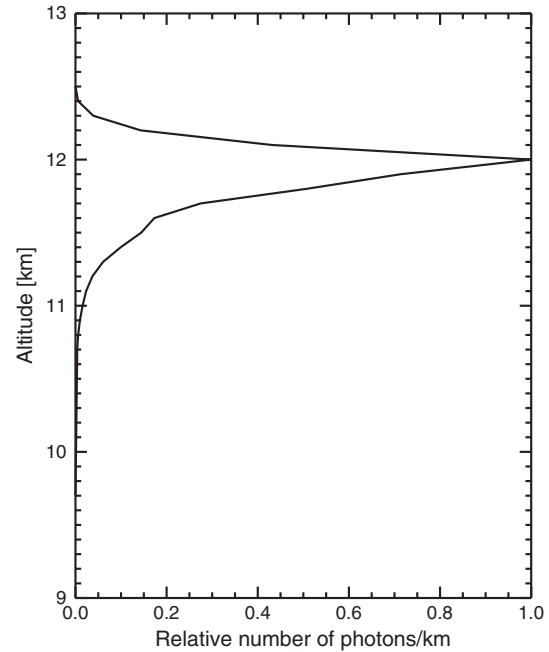


**Figure 1.** The altitude distribution from Smith [2011a] shown for an initial production altitude of 12 km. The photons are distributed over an atmospheric depth of 87 g/cm<sup>2</sup>.

spectrum one can get from bremsstrahlung and the cutoff corresponds to the largest single photon energy observed by AGILE [Marisaldi, 2010]. Tavani [2011] claim to have observed photons with energies up to 100 MeV, but the number of photons with these energies is very small. As the expected production altitude of TGFs is below 20 km, we have used initial production altitudes between 8 and 20 km. To be able to compare with earlier modeling results, we have also used both discrete and distributed photon production altitude distributions. For the distributed altitudes, we have used the distribution described in Smith [2011a] where the avalanche region extends over 87 g/cm<sup>2</sup> of air. Figure 1 shows the altitude distribution for a production altitude of 12 km and is taken directly from Smith [2011a]. For other altitudes, this distribution is scaled to stretch over 87 g/cm<sup>2</sup> at that specific altitude with the maximum of the distribution at the altitude in question. This means that the vertical length of the distribution is large for large initial altitudes and smaller for low initial altitudes. The distributed altitudes will be discussed below and our results will be compared with the results of Smith [2011a].

[10] We use three different angular distributions: (1) all photons distributed isotropically within a cone of  $\pm 30^\circ$  half angle, (2) distributed isotropically within  $\pm 40^\circ$  half angle, and (3) angular distributions out to  $90^\circ$  as shown in Figure 2a of Hazelton *et al.* [2009], all centered around the vertical direction. The angular distribution of Hazelton *et al.* [2009] was obtained from a model of the RREA with a vertical electric field and gave an energy-dependent angular distribution. For photons with energy less than 1 MeV, we have used the red distribution shown in Figure 2a of Hazelton *et al.* [2009]; for photons with energy more than 1 MeV, we have used the blue distribution in the same figure. Gjesteland *et al.* [2011] found all of these angular

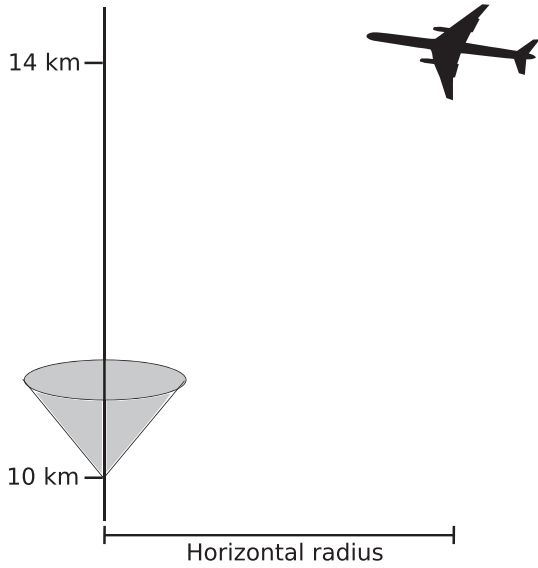


**Figure 2.** The geometry for the simulations. Horizontal radius is the distance from the initial photon production.

distributions to be consistent with observations. The photons going downward due to the feedback process described in Dwyer [2007, 2012] have been approximated by sending 0% (no feedback), 0.1% (weak feedback), or 1% (strong feedback) of the initial photons downward with the same initial angular distribution as the photons going upward. The fraction of photons initially traveling downward is determined by using the average number of downward traveling positrons produced per runaway electrons found by Dwyer [2012]. The number is found to be  $3 \times 10^{-4} \times r_n$  positrons per runaway electron per meter, where  $r_n$  is the number density of air relative to the ground. With electric field strengths just above the runaway threshold, around 30% of these positrons will turn around and be accelerated downward in the electric field [Dwyer, 2012, Figure B3]. The vertical field size needed to get an average RHESSI TGF is found by Dwyer and Smith [2005] to be of the order of 100 m/ $r_n$ . These numbers give about 1% photons initially traveling downward. The fraction of about 1% is also consistent with strong feedback in Figure 1 in Babich [2005].

[11] We have sampled all photons passing through detection altitudes of 14, 20 (aircraft altitudes), and 35 km (balloon altitude) and sorted them in intervals of 1 km horizontal radius from the initial position. The geometry is shown in Figure 2. The number of photons are then scaled according to the number of initial photons assumed.

### 3. Number of Initial Photons

[12] The number of initial photons in an average RHESSI TGF can be calculated semi-analytically. The average TGF detected by RHESSI has a fluence of  $\bar{I} = 0.1$  photons/cm<sup>2</sup> and RHESSI has been shown to see TGFs at least out to 600 km away from nadir [Cohen et al., 2010; Gjesteland et al., 2011; Collier et al., 2011]. The average fluence of photons in a circular area can be expressed as

$$\bar{I} = \frac{\int_0^{\theta_m} I(\theta) dA(\theta)}{\int_0^{\theta_m} dA(\theta)} \quad (1)$$

where  $I$  is the fluence at a given angle  $\theta$ ,  $dA$  is a small annular area at the angle  $\theta$ , and  $\theta_m$  is the maximum angle of observation. If we assume an isotropic initial angular distribution, the fluence is given as

$$I(\theta) = \frac{kI_0}{d^2} \quad (2)$$

where  $I_0$  is the initial number of photons per steradian,  $d = h/\cos \theta$  as shown in Figure 3, and  $k$  is a factor to account for the loss of photons in the atmosphere. From the geometry of the calculation shown in Figure 3, we get

$$dA = 2\pi a da = 2\pi h^2 \frac{\tan \theta}{\cos^2 \theta} d\theta \quad (3)$$

Solving these equations for  $I_0$ , we get

$$I_0 = \frac{\bar{I} h^2 \int_0^{\theta_m} \frac{\sin \theta}{\cos^3 \theta} d\theta}{k \int_0^{\theta_m} \tan \theta d\theta} \quad (4)$$

The total initial number of photons is then found by multiplying this with the solid angle:

$$N_0 = I_0 2\pi (1 - \cos \theta_m) \quad (5)$$

[13] The factor  $k$  is calculated from the Monte Carlo results as the relative number between the number of photons escaping the atmosphere to the number of initial photons. For each choice of initial parameters, we get a different  $k$ . The initial altitude distribution and the initial photon angular distribution give some contribution, but the main parameter is the production altitude. As we are only trying to determine the order of magnitude of  $k$ , we neglect other contributions than the initial production altitude. The values of  $k$  are in the range between  $10^{-2}$  and  $10^{-4}$  for altitudes from 20 km to 10 km. By using a discrete initial altitude distribution and the initial photon angular distribution of Hazelton et al. [2009, Figure 2a], we get a number of photons as given in Table 1.

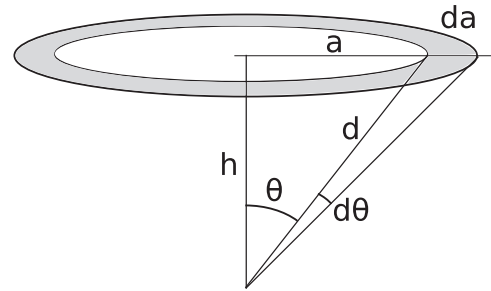


**Figure 3.** The geometry used for the calculation of number of initial photons.  $d$  is the distance between the initial photon production and the satellite,  $h$  is the difference in altitude between the initial photon production and the satellite, and  $\theta$  is the angle between  $h$  and  $d$ .

**Table 1.** Number of Initial Photons for Different Initial Production Altitudes

Initial Photon Altitude	Number of Initial Photons
10 km	$10^{18}$
15 km	$10^{17}$
20 km	$10^{16}$

[14] As seen in Table 1, the initial production altitude gives a large variation in the number of initial photons needed to match the average intensities observed by RHESSI. These numbers are calculated with  $\theta_m = 45^\circ$ , and the result is sensitive to the choice of this parameter. TGFs have been observed out to  $\theta_m = 60^\circ$  [Cohen *et al.*, 2010] but the small number of TGFs at these large angles may suggest that these TGFs are especially strong. If we use  $\theta_m = 60^\circ$ , the number of initial photons increase with a factor of 2–3. When using a distributed initial production altitude distribution, the number of initial photons increases by approximately 10%. A change in the initial photon angular distribution gives an increase of up to 20%, while varying the production altitude gives variations of a factor of 10 and 100.

#### 4. Dependence on Initial Conditions

[15] For the simulations presented in the beginning of this section, we have used an initial number of photons of  $10^{17}$ , of which  $10^8$  are simulated and then scaled with  $10^9$ . This corresponds to a production altitude of 15 km for an average RHESSI TGF and is the most used number of initial photons in other models [Dwyer, 2012]. The results when using different number of initial photons for the different initial altitudes are shown at the end of the section.

[16] The initial production altitude of the photons is very important due to the attenuation in the dense lower atmosphere. As shown in Figure 4, the difference in fluence when observed at 35 km varies 2–3 orders of magnitude when assuming production altitudes from 10 km to 20 km. For observations at 14 km and 20 km, some of the initial production altitudes will be below the observation altitude and

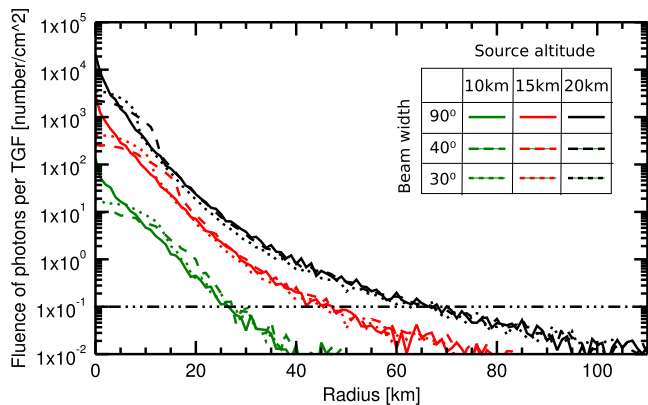


**Figure 4.** Fluence of photons at 35 km altitude. The detection threshold is set to 300 keV, the initial number of photons is  $10^{17}$ , and the initial photon altitude distribution is discrete. The drop in the two isotropic angular distributions is due to the effect of being inside or outside of the initial cone.

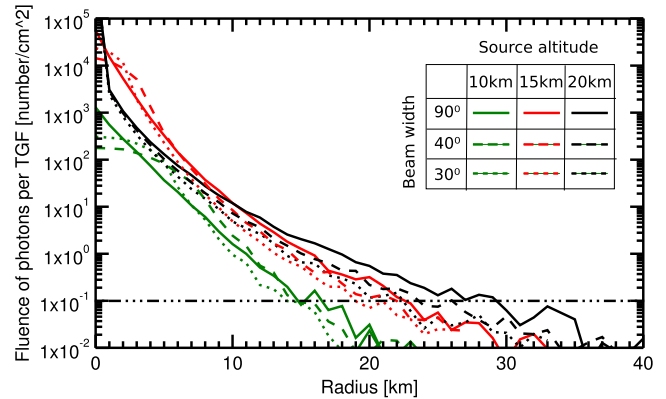


**Figure 5.** Fluence of photons at 20 km altitude. The detection threshold is set to 300 keV, the initial number of photons is  $10^{17}$ , and the initial photon altitude distribution is discrete.

some will be at the same altitude or above. The fluence of photons is then highly dependent on the other initial conditions. Figure 4 also shows how the fluence varies with initial angular distribution. As long as the observation altitude is higher than the initial production altitude, the main difference between the initial angular distributions is that the two isotropic distributions give a clear drop in fluence around the maximum angle of  $30^\circ$  or  $40^\circ$ . This is an effect of observing inside or outside the initial cone of the photon angular distribution. When the photons are distributed smoothly out to  $90^\circ$ , there is no such cutoff. For horizontal distances larger than where we see the drop off distance, the fluence for all angular distributions is similar.

[17] As long as the TGFs are observed above the initial production altitude, the fluence does not depend significantly on the initial production altitude distribution (not shown). For isotropic initial angular photon distribution, the drop at  $30^\circ$  or  $40^\circ$  half angle is sharper for a discrete initial production altitude than for a distributed initial production altitude. The effect of feedback is also small for observational altitudes higher than the initial production altitude.

[18] Figure 5 is fluence for observation at 20 km altitude and shows the same features as commented in connection to observations at 35 km altitudes. For production at 20 km altitude (black curve), we see that the differences between the initial photon angular distributions are small. Hence, the number of backscattered photons is quite similar for the three different cases.

[19] Figure 6 shows the fluence of photons at 14 km. Observations at this altitude show a large difference between observations above or below the initial production altitude of the TGF. The photons below the initial production altitudes consist of photons being Compton scattered down and photons produced by positrons moving down. In the process of Compton scattering, the photons will in general lose much of their energy. As seen in the figure, the fluence from a TGF produced at 20 km is much smaller than for production closer to the observational altitude. Here, the solid lines are for production at discrete altitude and the dashed lines are for distributed initial altitudes. A distributed initial production altitude gives a slightly larger fluence when the observations are made below the initial production altitude. This will be discussed below. The difference between

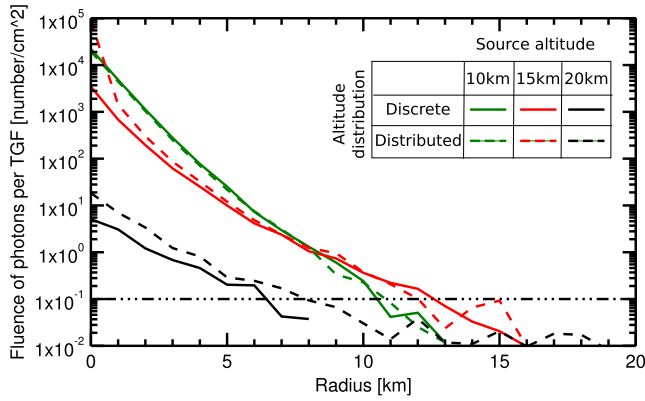


**Figure 6.** Fluence of photons at 14 km altitude. The detection threshold is 300 keV, the initial number of photons is  $10^{17}$ , and the photons have an initial angular distribution out to  $90^\circ$ . The TGFs with distributed altitudes are distributed according to Figure 1.

distributed and discrete altitudes for TGFs produced at 10 km and 15 km is small. This is because the distributed altitudes have a very narrow peak which means that the main part of the photons are originating close to the maximum altitude of the distribution.

[20] Figure 7 shows the effect of feedback when the observations are made below the initial production altitude. At these observational altitudes, even a small feedback will give a larger fluence than with no feedback, and an increased feedback will increase the fluence significantly. The fluence falls off somewhat faster with radial distance when feedback is included. All the profiles are for discrete production altitudes, and the differences are larger for discrete altitudes than for distributed altitudes.

[21] When observing from below the production altitude, the drop at  $30^\circ$  or  $40^\circ$  half angles is only seen when feedback is included. This is an effect of using the same initial photon angular distributions for photons going downward and upward. For the TGF originating at 15 km altitude, the

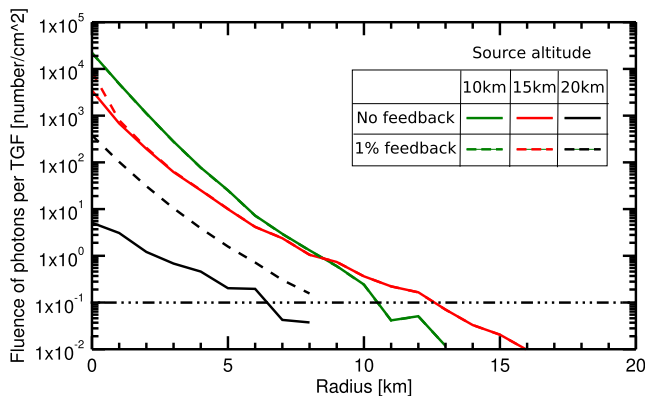


**Figure 7.** Fluence of photons at 14 km altitude. The detection threshold is 300 keV, the initial number of photons is  $10^{17}$ , the photons have an initial angular distribution out to  $90^\circ$ , and the initial photon altitude distribution is discrete. Feedback is approximated by giving 1% of the photons an initial downward direction, see section 5 for discussion.

**Table 2.** Maximum Radius of Detection of All the Various TGFs Modeled in This Work<sup>a</sup>

Detection Altitude	Unscaled		Scaled	
	300 keV	100 keV	300 keV	100 keV
14 km	6 km	8 km	3 km	6 km
20 km	14 km	19 km	18 km	23 km
35 km	27 km	32 km	39 km	51 km

<sup>a</sup>Unscaled is maximum radius for a TGF with  $10^{17}$  initial photons at all altitudes, scaled is for TGFs initial number of photons scaled according to Table 1. The maximum radius is given for instruments with a low energy threshold of 100 keV and 300 keV.

main part of the observed photons is backscattered photons originally directed upward. This makes the intensity difference between TGFs with and without feedback very small at radial distances larger than about 1 km.

[22] What mostly affects the ability to detect TGFs at different observational altitudes is the maximum horizontal distance of detection. Table 2 shows the maximum horizontal distance from the source at which the instrument can still detect all the various TGFs, independent of initial conditions, within the constraints of this paper. In other words, we have used the initial conditions that give the smallest fluence at the observational altitude in consideration. The instrument is assumed to have a detection limit of 0.1 photon/cm<sup>2</sup>. With an energy threshold of 300 keV, the instrument can detect all the various TGFs within a radial distance of 27 km when observed at 35 km altitude. At 20 km altitude, the maximum radial distance is 14 km, and at 14 km altitude maximum distance is 6 km.

[23] Another major difference is the change between observing the TGF from a position above or below the altitude where the TGF originates. When observed at 14 km altitude, the probability of detection is highly affected by the amount of feedback and the altitude distribution of the initial photons. The fluence of photons is much smaller with no or weak feedback (0.1%), than with an average feedback (1%) or more, which also makes the maximum radius of detection much smaller. This is further discussed below.

[24] With a decreasing lower energy threshold from  $E > 300$  keV to  $E > 100$  keV, the fluence and the maximum radial distance of detection increase. This is shown in Table 2. The increased number of photons is most important at large radial distances where the relative number of low energy photons to high energy photons is largest. When the photons are distributed out to  $30^\circ$  or  $40^\circ$ , all photons detected at large angles/large horizontal distance have experienced Compton scattering and lost energy [Østgaard *et al.*, 2008; Hazelton *et al.*, 2009]. Thus, we see a larger number of high energy photons at large distances when the photons are distributed out to  $90^\circ$ .

#### 4.1. Differentiated Number of Initial Photons

[25] Table 2 and Figure 8 show the maximum radius of observation and fluence at 35 km altitude when we use  $10^{16}$  initial photons for a TGF originating at 20 km altitude,  $10^{17}$  initial photons for a TGF produced at 15 km altitude, and  $10^{18}$  initial photons for a TGF produced at 10 km altitude. Figure 8 shows that the fluence of photons is about similar when using differentiated number of initial photons. This is because the number of photons is calculated to match the average RHESSI TGF, and the fluence of photons at a given

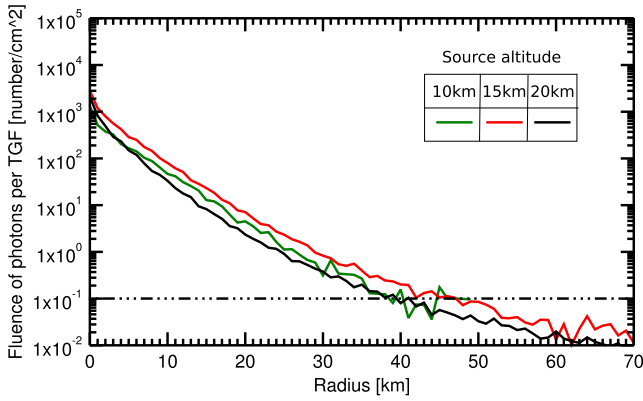


**Figure 8.** Fluence of photons at 35 km altitude. The detection threshold is set to 300 keV and the initial photon altitude distribution is discrete. The number of initial photons is scaled according to Table 1.

altitude should then be the same for all initial production altitudes. If we had used the exact number from the calculation, instead of order of magnitude, all three curves should be equal. This also underlines that the number of initial photons is an important parameter for simulations of TGFs and that the production altitude is the main parameter determining the final flux.

## 5. Discussion

[26] To compare our results with the results of *Smith* [2011a], we have distributed the initial photons over  $87 \text{ g/cm}^2$  of atmosphere. At 8 km altitude, this corresponds to a vertical distance of 1500 m. Due to the exponential decrease in density of the atmosphere with altitude, this vertical distance will increase for higher altitudes. At 20 km altitude, the photons are distributed over 5800 m vertical distance with the top of the distribution at 20 km. Using balloon measurements of electric fields in thunderstorms, *Marshall*

*et al.* [2005] show the existence of electric fields larger than the limit for relativistic breakdown only extend over  $\sim 1 \text{ km}$  at 6 km altitude. This corresponds to an atmospheric depth of  $70 \text{ g/cm}^2$ , which is comparable to a 5 km vertical extension of the electric field at 20 km altitude. In balloon observations reported by *Stolzenburg et al.* [2007], from several observations at higher altitudes, the electric field seems to extend over even smaller vertical distances.

[27] Having electric fields at the threshold for RREA over an atmospheric depth of  $87 \text{ g/cm}^2$  implies a potential difference of 200 MV for any altitude. This is the lower limit for the production of high energy photons across the whole vertical distance used as the distributed altitudes in our modeling. From balloon soundings, the potential between the nearest relative maximum and minimum potential in thunderclouds was reported by *Marshall and Stolzenburg* [2001] to be up to  $132 \pm 2 \text{ MV}$ . Most thunderclouds are therefore not expected to have potentials of more than 200 MV which is required for RREA over  $87 \text{ g/cm}^2$ . As the altitude distribution in *Smith* [2011a] is derived from the assumption of a very powerful thunderstorm, they probably overestimate the feedback factor as well as the prediction of seeing TGFs by letting the photons being produced over a too large altitude range.

[28] A consequence of having electric fields over large vertical distances is that at least 10% of the photons will have initial production altitudes lower than 15 km for all the different initial altitudes. This also explains the difference between discrete and distributed initial production altitudes for observations in 14 km altitude in our results.

[29] Figure 9 shows a comparison between our results and Figure 1 in *Smith* [2011a]. The figure of *Smith* [2011a] gives the contours for 20, 200, 2000, and 20,000 counts in the detector used by ADELE. We have not been able to propagate out photons through the aircraft body, which means that we overestimate the number of photons. We have used an effective area of the detector of  $65 \text{ cm}^2$  [*Smith*, 2011a].

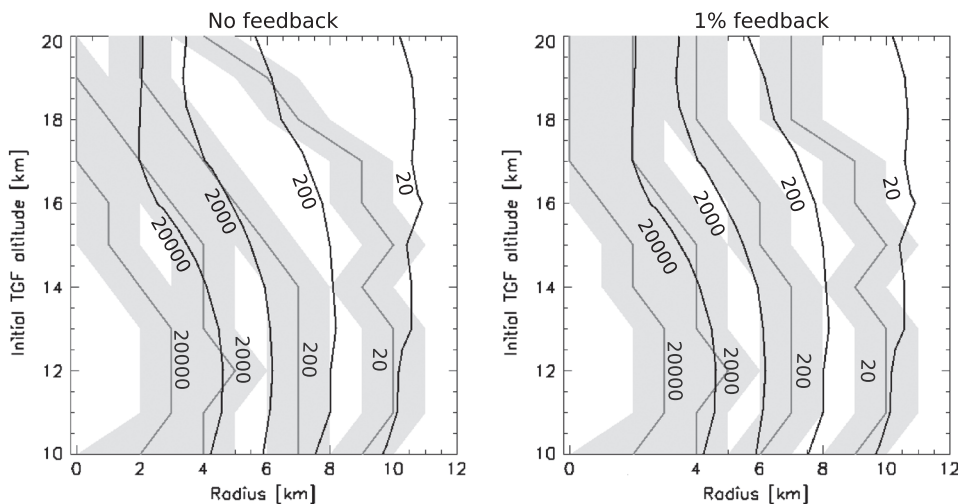


**Figure 9.** Contours of counts in the detector used by ADELE [*Smith*, 2011a]. The black curves are results from *Smith* [2011a], and the gray curves are our results including error bars. The left figure shows our results without feedback and the right figure is with 1% feedback. The curves are for an observational altitude of 14 km, with initial production altitudes distributed over  $87 \text{ g/cm}^2$  and initial production angles out to  $90^\circ$ .

In Figure 9, the results of *Smith* [2011a] are shown in black and our results are shown in gray with error bars. As we calculate the flux of photons at every kilometer radius, we will have an error of  $\pm 1$  km. The figure on the left shows our results without feedback and the figure to the right shows the results with 1% feedback. Without feedback, our contours drop faster to 0 radius at high production altitudes compared to *Smith* [2011a]. With 1% feedback, the curves are more similar, but we have to include 5% feedback to be able to replicate the shape of the contours from *Smith* [2011a]. However, we are not able to replicate the distances that are shown by *Smith* [2011a]. The main difference in our simulations and the simulations of *Smith* [2011a] is the energy-angle distribution. We assumed the same energy distribution for the downward running photons produced by feedback as the upward moving photons. Then we have implemented the energy-dependent angular distribution of *Hazelton et al.* [2009] by distributing all energies  $>1$  MeV according to Figure 2a in *Hazelton et al.* [2009], but have neglected that the high energy part of the photon spectrum has a narrower angular distribution. Hence, the high energy photons in our model is distributed more widely than is the case in *Hazelton et al.* [2009] and *Smith* [2011a]. This results in a small bias toward larger observational distances in our results.

[30] The results in this paper are based on the intensities of an average TGF. However, according to *Østgaard et al.* [2012], one can expect a large number of TGFs with lower initial intensity. For these TGFs, the maximum radius of detection will be even smaller. ADELE had 133 discharges closer than 4 km to the aircraft. The results of our simulations show that if the assumptions made by *Smith* [2011a] are valid then the non-detection of ADELE means that TGFs are rare events. However, if the TGFs are produced in a shorter altitude interval and with less feedback, or with lower intensities than an average RHESSI TGF, then the TGFs might not be detectable to ADELE even at small radial distances. The results presented here combined with the fluence distribution found by *Østgaard et al.* [2012] makes it very likely that all the 133 discharges closer than 4 km from ADELE were low fluence TGFs that did not produce detectable signal for ADELE. Furthermore, our results support the conclusion by *Gjesteland et al.* [2012] and *Østgaard et al.* [2012] that TGFs probably are a more common phenomenon than previously reported.

## 6. Conclusion

[31] In this paper we have shown how simulations of photon fluence at aircraft and balloon altitudes depend on the initial conditions. For all observational altitudes the number of photons and the initial production altitude are the two main parameters. When observations are made below the initial production altitude of the TGF, other parameters such as initial production altitude distribution, initial photon angular distribution and amount of feedback also give large differences. This means that one have to be careful when making conclusions based on these type of simulations. The comparisons to the non detection of ADELE together with the results of *Østgaard et al.* [2012] support the possibility that all discharges may produce TGFs.

[32] **Acknowledgment.** This study was supported by the Norwegian Research Council under contract 208028/F50.

## References

- Babich, L. P. (2005), The feedback mechanism of runaway air breakdown, *Geophys. Res. Lett.*, *32*(9), 1–5, doi:10.1029/2004GL021744.
- Briggs, M. S., et al. (2010), First results on terrestrial gamma ray flashes from the Fermi gamma-ray burst monitor, *J. Geophys. Res.*, *115*(A7), 1–14, doi:10.1029/2009JA015242.
- Cohen, M. B., U. S. Inan, R. K. Said, and T. Gjestland (2010), Geolocation of terrestrial gamma-ray flash source lightning, *Geophys. Res. Lett.*, *37*(2), 1–5, doi:10.1029/2009GL041753.
- Collier, A. B., T. Gjesteland, and N. Østgaard (2011), Assessing the power law distribution of TGFs, *J. Geophys. Res.*, *116*(A10), A10,320, doi:10.1029/2011JA016612.
- Dwyer, J. R. (2007), Relativistic breakdown in planetary atmospheres, *Phys. Plasmas*, *14*(4), 042,901, doi:10.1063/1.2709652.
- Dwyer, J. R. (2012), The relativistic feedback discharge model of terrestrial gamma ray flashes, *J. Geophys. Res.*, *117*(A2), A02,308, doi:10.1029/2011JA017160.
- Dwyer, J. R., and D. M. Smith (2005), A comparison between Monte Carlo simulations of runaway breakdown and terrestrial gamma-ray flash observations, *Geophys. Res. Lett.*, *32*(22), 1–4, doi:10.1029/2005GL023848.
- Fishman, A. G. J., et al. (1994), Discovery of intense gamma-ray flashes of atmospheric origin, *Adv. Sci.*, *264*(5163), 1313–1316.
- Gjesteland, T., N. Østgaard, P. H. Connell, J. Stadsnes, and G. J. Fishman (2010), Effects of dead time losses on terrestrial gamma ray flash measurements with the burst and transient source experiment, *J. Geophys. Res.*, *115*, 1–10, doi:10.1029/2009JA014578.
- Gjesteland, T., N. Østgaard, A. B. Collier, B. E. Carlson, M. B. Cohen, and N. G. Lehtinen (2011), Confining the angular distribution of terrestrial gamma-ray flash emission, *J. Geophys. Res.*, *116*(A11), A11,313, doi:10.1029/2011JA016716.
- Gjesteland, T., N. Østgaard, A. B. Collier, B. E. Carlson, C. Eyles, and D. M. Smith (2012), A new method reveals more TGFs in the RHESSI data, *Geophys. Res. Lett.*, *39*(5), 1–5, doi:10.1029/2012GL050899.
- Hazelton, B. J., B. W. Grefenstette, D. M. Smith, J. R. Dwyer, X.-M. Shao, S. A. Cummer, T. Chronis, E. H. Lay, and R. H. Holzworth (2009), Spectral dependence of terrestrial gamma-ray flashes on source distance, *Geophys. Res. Lett.*, *36*(1), 1–5, doi:10.1029/2008GL035906.
- Inan, U. S., S. C. Reising, G. J. Fishman, and J. M. Horack (1996), On the association of terrestrial gamma-ray bursts with lightning and implications for sprites, *Geophys. Res. Lett.*, *23*(9), 1017, doi:10.1029/96GL00746.
- Marisaldi, M., et al. (2010), Detection of terrestrial gamma ray flashes up to 40 MeV by the AGILE satellite, *J. Geophys. Res.*, *115*, 1–12, doi:10.1029/2009JA014502.
- Marshall, T. C., and M. Stolzenburg (2001), Voltages inside and just above thunderstorms, *J. Geophys. Res.*, *106*(D5), 4757–4768, doi:10.1029/2000JD900640.
- Marshall, T. C., M. Stolzenburg, C. R. Maggio, L. M. Coleman, P. R. Krehbiel, T. Hamlin, R. J. Thomas, and W. Rison (2005), Observed electric fields associated with lightning initiation, *Geophys. Res. Lett.*, *32*(3), 1–5, doi:10.1029/2004GL021802.
- Østgaard, N., T. Gjesteland, J. Stadsnes, P. H. Connell, and B. Carlson (2008), Production altitude and time delays of the terrestrial gamma flashes: Revisiting the burst and transient source experiment spectra, *J. Geophys. Res.*, *113*(A2), 1–14, doi:10.1029/2007JA012618.
- Østgaard, N., T. Gjesteland, R. S. Hansen, A. B. Collier, and B. Carlson (2012), The true fluence distribution of terrestrial gamma flashes at satellite altitude, *J. Geophys. Res.*, *117*(A3), A03,327, doi:10.1029/2011JA017365.
- Shao, X.-M., T. Hamlin, and D. M. Smith (2010), A closer examination of terrestrial gamma-ray flash-related lightning processes, *J. Geophys. Res.*, *115*(April 2004), 1–8, doi:10.1029/2009JA014835.
- Smith, D. M., L. I. Lopez, R. P. Lin, and C. P. Barrington-Leigh (2005), Terrestrial gamma-ray flashes observed up to 20 MeV, *Science (New York, N.Y.)*, *307*(5712), 1085–1088, doi:10.1126/science.1107466.
- Smith, D. M., et al. (2011a), The rarity of terrestrial gamma-ray flashes, *Geophys. Res. Lett.*, *38*(8), 3–7, doi:10.1029/2011GL046875.
- Smith, D. M., et al. (2011b), A terrestrial gamma-ray flash observed from an aircraft, *J. Geophys. Res.*, *116*(D20), D20,124, doi:10.1029/2011JD016252.
- Stolzenburg, M., T. C. Marshall, W. D. Rust, E. Bruning, D. R. Macgorman, and T. Hamlin (2007), Electric field values observed near lightning flash initiations, *Geophys. Res. Lett.*, *34*, 1–7, doi:10.1029/2006GL028777.
- Tavani, M., et al. (2011), Terrestrial gamma-ray flashes as powerful particle accelerators, *Phys. Rev. Lett.*, *106*(1), 1–5, doi:10.1103/PhysRevLett.106.018501.